

Correlation between Lattice Constant, Bulk Density and Dielectric Loss of Nanocrystalline spinel Ferrite Material due to Doping Effect of Ni^{2+} , Co^{2+} and Cu^{2+} in CuCo, NiCu and CoNi respectively using Sol Gel Method.

A.M. Tamboli¹, Dr. Gulam Rabbani², Dr. S. M. Rathod³, Dr. Azhar M Shaikh⁴

Associate Professor, Department of Electronic Science, Poona College, Pune, Maharashtra, India¹.

Director, Dr. Rafiq Zakaria Center for Higher Learning and Advance Research, Aurangabad,
Maharashtra, India².

Associate Professor, Department of Physics, Abasaheb Garware College, Pune, Maharashtra, India³.

Assistant Professor, Department of Physics, Sir Sayyed College of Arts, Commerce and Science, Roshan Gate
Aurangabad, Maharashtra, India⁴.

ABSTRACT: The preparation of ferrite materials by using SOL-GEL Auto Combustion Technique is explained and importance of Nanocrystalline spinel ferrite material. Structural characterization of the annealed samples of ferrite material at 400°C for 4 hours is done by using X-ray diffraction method (XRD). The single phase formation of $\text{NiCuCoFe}_2\text{O}_4$ ferrite material is confirmed by X-ray diffraction analysis by using Braggs Law. XRD revealed that the average crystalline particle size which was calculated by using Scherer method is between 20 to 30 nm. The lattice constant is calculated by using proper formula. The pellets of ferrite material are made by adding polyvinyl alcohol (PVA) as binder in powder of ferrite material. Impedance meter, LCR-Q meter is used to calculate the Dielectric Loss in the frequency range of 100 Hz to 5 MHz at room temperature. The change in Lattice constant is observed due to doping of Ni^{2+} , Co^{2+} and Cu^{2+} in CuCo, NiCu and CoNi respectively. The correlation ship between the Lattice constant, Bulk Density and Dielectric Loss ($\tan \delta$) of Nanocrystalline spinel Ferrite Material is discussed.

KEYWORDS: Sol-gel auto-combustion, X-ray diffraction (XRD), LCR-Q Meter.

I. INTRODUCTION

The properties of material changes at nanoscale and certain properties such as physical, electric, Magnetic and Dielectric properties of Nanocrystalline ferrite Material change drastically at nano scale. The ability to produce nanosized due to small grain size which changes the physical, electric, Magnetic, Dielectric and resistivity properties of Nanocrystalline ferrite Material opened new application for materials such as Electromagnetic wave absorber, magnetic data storage, strong in electronic appliance, Ferro fluid technology, gas sensors, magnetically targeted drug carriers, filters in electronic communication and agents in magnetic resonance imaging.

The Nanocrystalline ferrite Material is form an important class of Nanocrystalline materials because of their low weigh, high resistivity, long life, low cost of preparation and low energy losses (eddy current). It plays important

International Journal of Innovative Research in Science, Engineering and Technology

(An ISO 3297: 2007 Certified Organization)

Website: www.ijirset.com

Vol. 6, Issue 7, July 2017

role in technological application over wide range of frequencies [1-3]. Recent studies have shown that the physical properties of nanoparticles are influenced significantly by the processing technique [4-6]. Since crystallite size, distribution of particle sizes and inter particle spacing have the greatest impact on Dielectric properties such as Dielectric loss and AC Conductivity. Many wet-chemical methods are employed for the preparation of the nano-sized spinel ferrite. One of them is sol-gel auto combustion which has recently become very popular technique. It is a simple process, which offers significant saving in time, electricity and Money as compare to other traditional methods and it also requires a low sintering temperature. Sol gel method is used to obtain better physical properties, more homogeneity and narrow particle size distribution thereby influencing structural, electrical and Dielectric properties of Nanocrystalline ferrite Material [7-9]. It is well known that, some magnetic properties such as saturation magnetization and Coercivity and some Dielectric properties such as Dielectric loss tangent ($\tan \delta$), AC electrical conductivity (σ_{ac}) and Dielectric constant (Real Part= ϵ') depend strongly on Lattice constant, Bulk Density, particle size and microstructure of the materials. Therefore, it is interesting and important thing to develop the various techniques by which the size and shape of the particles can be well controlled. One of the ways to prepare the nanocrystalline spinel ferrite material with required properties is Sol-gel auto combustion technique. In the present work we have systematically studied the effect of doping of Ni^{2+} , Co^{2+} and Cu^{2+} in CuCo, NiCu and CoNi respectively on Lattice Constant, Bulk Density and Dielectric Loss($\tan \delta$) of Nanocrystalline spinel Ferrite Material.

II. RELATED WORK

2.1. Experimental technique

In sol-gel auto combustion synthesis technique, high purity AR grade chemicals such as ferric nitrate ($Fe(NO_3)_3 \cdot 9H_2O$), Copper nitrate ($Cu(NO_3)_2 \cdot 6H_2O$), Nickel nitrate ($Ni(NO_3)_2 \cdot 6H_2O$), Cobalt nitrate ($Co(NO_3)_2 \cdot 6H_2O$), citric acid ($C_6H_8O_7$), ammonium hydroxide solution (NH_4OH) were used to prepare the series of $[(Ni_{0.2} Cu_{0.2} Co_{0.6})Fe_2O_4]$, $[(Ni_{0.4} Cu_{0.2} Co_{0.4})Fe_2O_4]$, $[(Ni_{0.6} Cu_{0.2} Co_{0.2})Fe_2O_4]$, $[(Ni_{0.2} Cu_{0.6} Co_{0.2})Fe_2O_4]$, $[(Ni_{0.2} Cu_{0.4} Co_{0.4})Fe_2O_4]$ and $[(Ni_{0.4} Cu_{0.4} Co_{0.2})Fe_2O_4]$ Nano crystalline ferrite materials. In this chemical process Citric acid was used as a Fuel [8-10]. These nitrates and citric acid were weighed accurately to have proper stoichiometric proportion required in the final product. The mixed solutions of all the chemicals were stirred until the homogeneous solution is obtained. During the stirring process ammonium hydroxide solution was added drop by drop to obtain pH of 7. The mixed solution was simultaneously heated at $100^\circ C$ for 3 to 4 h to form sol. The transparent sol was further heated at $100^\circ C$ for 2 h for removal of water. The sol turns into a viscous brown gel. The temperature of the gel was further increased up to $120^\circ C$, after some time combustion of the gel takes place and fine powder of ferrite nanoparticles was obtained. The ferrite powder was sintered at $400^\circ C$ for 4 hours in air medium to get better crystallization and homogeneous distribution in the spinel and finally ground to get the series of Nano crystalline ferrite material. Table 1 indicates Label and composition for the series of ferrite materials of all six reactions which is divided in to three Sets. Table 2 indicates the values of Lattice Constant, Bulk Density and Dielectric Loss ($\tan \delta$) of all six Nanocrystalline spinel Ferrite Material prepared by Sol Gel Method. Fig. 1 shows the Sol gel auto combustion synthesis used for the preparation of the ferrite powders.

2.2. Perpetration and Sintering of pellets

The pellets are prepared by mixing the polyvinyl alcohol (PVA) as binder in to ferrite powder. The mixed powder was uniaxially pressed by using a hydraulic press machine by applying the pressure of about 60 kg/cm^3 for about 1 minute in a die of 10mm diameter. The final sintering of pellets was carried out at $200^\circ C$ for about 2 hours in air medium to densify the pellets. The pellets of diameter D_0 -10 mm, thickness-2 mm are fabricated. The prepared samples of pellets were sintered in a furnace which uses electricity for heating the chamber with the help of super kanthal ($MoSi_2$) heating elements and alumina insulation boards as chamber walls. The dimension of chamber is $250 \times 150 \times 150 \text{ mm}$. The thermal regime of the furnace was controlled through a "Eurotherm" programmer-cum-controller designed by using microcontroller with an accuracy of $\pm 2^\circ C$. The compacted samples heated from room

International Journal of Innovative Research in Science, Engineering and Technology

(An ISO 3297: 2007 Certified Organization)

Website: www.ijirset.com

Vol. 6, Issue 7, July 2017

temperature to 200°C at a rate 1°C/min followed by a soaking at 200°C for 2 hours for binder burnout.

2.3. Characterization of Lattice constant, Bulk Density and Dielectric Loss

Using the XRD data, the interplaner spacing 'd' values for all the reflections were determined using Bragg's law. The bulk density of all nanocrystalline spinel ferrite material is measured by using Archimedes principle [10-11].

Lattices Constant (Å) is calculated by using the formula $\frac{1}{d^2} = \frac{1}{a^2 \times (h^2 + k^2 + l^2)}$ – (1)

The Dielectric Loss of prepared samples was measured in the frequency range of 100 Hz to 5 MHz by using impedance analyser (LCR-Q Meter) meter at room temperature. The data acquisition system of digital impedance analyser (LCR-Q meter) provides the information of applied frequency (f), and Quality factor (Q).

Dielectric loss tangent= (tan δ) = 1/Q – (2)

III. RESULTS AND DISCUSSION

3.1. X-ray diffraction pattern

Fig. 2 shows the X-ray diffraction pattern of A, B, C, D & F. Its compositions exhibit single phase cubic spinel structure with $Fd\bar{3}m$ space group and there is not presence of any secondary phase. All the reflections are slightly broader and less intense which indicate the nanocrystalline nature of the samples. The analysis of X-ray diffraction pattern revealed that all the samples under investigation possess single phase cubic spinel structure.

3.2. Effect of Ni^{2+} substitution on Lattice Constant, Bulk Density and Dielectric Loss (tan δ).

Due to the doping of Ni^{2+} ions in place of Co^{2+} ions, it is observe that Bragg's angle shifts towards higher angle and thereby interplaner spacing 'd' values decreases. It is observe that lattice constant decreases with increase in Ni^{2+} doping from x=0.2 to x=0.6. The variations in lattice constant as a function of Nickel concentration x can be understood on the basis of the ionic radius of doped cations. The ionic radius of Ni^{2+} ions (0.69Å) is less than that of Co^{2+} ions (0.72Å) therefore due to effect of doping the lattice constant expected to decrease with increase in Ni^{2+} concentration of doping. When the smaller nickel ions enters the lattice unit cell expands while preserving overall symmetry this is true as long as the lattice constant decreases with doping concentration of Ni^{2+} and obeys Vegard's law [12-16]. Fig 3 shows the decrease in the value of Lattice constant with the increase in Ni^{2+} concentration of doping. From Fig. 5 it is observed that due to increase of Ni^{2+} doping from 0.2 to 0.4 Bulk Density decreases and thereafter Bulk Density increases with further increase in doping of Ni^{2+} ions from 0.4 to 0.6. The

The average Dielectric Loss (tan δ) all ferrite samples due to Ni^{2+} doping is calculated in the frequency range of 100 Hz to 5 MHz. From Fig. 4 it is observed that due to increase of Ni^{2+} doping from 0.2 to 0.6, average Dielectric Loss (tan δ) decreases. Fig 3 and Fig 4 show the correlation between lattice constant and average Dielectric Loss (tan δ), both decreases with increase of Ni^{2+} ions doping from 0.2 to 0.6.

Table 3 indicates the values of Lattice Constant, Bulk Density and Dielectric Loss (tan δ) of Nanocrystalline spinel Ferrite Material in SET-I, namely A, B and C.

The properties of Dielectric material are it is insulator and it gets charged when it is placed under the influence of electric field [17-19]. The decrease in Dielectric Loss (tan δ) may be due to Vander walls equation effect. The increase in the concentration of Ni^{2+} ions at octahedral (B) site causes the migration of Fe^{3+} ions to tetrahedral (A) site.

International Journal of Innovative Research in Science, Engineering and Technology

(An ISO 3297: 2007 Certified Organization)

Website: www.ijirset.com

Vol. 6, Issue 7, July 2017

This increased concentration of Fe^{3+} ions increases the hopping rate of electrons between Fe^{3+} and Fe^{2+} ions at tetrahedral (A) site and thus leads to decrease the Dielectric Loss ($\tan \delta$).

3.3. Effect of Co^{2+} substitution on Lattice Constant, Bulk Density and Dielectric Loss ($\tan \delta$).

It is observed that due to the inclusion of Co^{2+} ions in place of Cu^{2+} ions the Bragg's angle shifts towards lower angle and lattice constant found to increase with increase in Co^{2+} ions doping from $x=0.2$ to 0.6 . The variations in lattice constant as a function of Cobalt ions doping concentration x can be understood on the basis of the ionic radius of the doped cations. The ionic radius of Co^{2+} ions (0.745\AA) is greater than that of Cu^{2+} ions (0.73\AA), therefore it is expected to increase the lattice constant with increase in Cobalt doping x [20-22]. When the larger Cobalt ions enters, the lattice unit cell expands while preserving overall symmetry this is true as long as the lattice constant increases with substituent concentration of Cobalt [23-24].

Fig 6 shows the increase in the value of Lattice constant with the increase in doping concentration of Co^{2+} . Fig 7 it is observe that Bulk Density increases with the increase in doping concentration of Co^{2+} from $x=0.2$ to $x=0.6$. From Fig. 8 it is observed that due to increase of Co^{2+} doping from 0.2 to 0.4 average Dielectric Loss ($\tan \delta$) increases and thereafter average Dielectric Loss ($\tan \delta$) decreases with further increase in doping of Co^{2+} ions from 0.4 to 0.6 .

Fig 6 and Fig 7 show the correlation between lattice constant and Bulk density, both increases with the increase of Co^{2+} ions doping from 0.2 to 0.6 . Table 4 indicates the values of Lattice Constant, Bulk Density and Dielectric Loss ($\tan \delta$) of Nanocrystalline spinel Ferrite Material in SET-II, namely D, E and A.

3.4. Effect of Cu^{2+} substitution on Lattice Constant, Bulk Density and Dielectric Loss ($\tan \delta$).

It is observed that Lattice constant gets affected due to the doping of Cu^{2+} ions in place of Ni^{2+} ions. Due to doping of Cu^{2+} ions from 0.2 to 0.4 the Bragg's angle shifts towards lower angle and Lattice constant is found to increase with increase in Cu^{2+} doping from 0.2 to 0.4 . But due to further doping of Cu^{2+} from $x=0.4$ to $x=0.6$ Bragg's angle shifts towards higher angle which causes to decrease the Lattice constant.

The variations in lattice constant as a function of Copper concentration x can be understood on the basis of the ionic radius of the substituted cations. Since the ionic radius of Cu^{2+} ions (0.73\AA) is greater than that of Ni^{2+} ions (0.69\AA), the substitution is expected to increase the lattice constant with increase in Copper concentration x [25-26]. When the larger Copper ions enter, the lattice unit cell expands while preserving overall symmetry this is true as long as the lattice constant increases with substituent concentration of Copper.

Fig. 9, Fig. 10 and Fig. 11 it is observed that due to increase of Cu^{2+} doping from 0.2 to 0.4 Lattice constant, average Dielectric Loss ($\tan \delta$) and Bulk density increases and thereafter Lattice constant, average Dielectric Loss ($\tan \delta$) and Bulk density decreases with further increase in doping of Cu^{2+} ions from 0.4 to 0.6 .

Table 5 indicates the values of Lattice Constant, Bulk Density and Dielectric Loss ($\tan \delta$) of Nanocrystalline spinel Ferrite Material in SET-III, namely C, F and D.

The increase in the concentration of Cu^{2+} ions at the tetrahedral (A) site causes the migration of Fe^{3+} ions to octahedral (B) site. This increased concentration of Fe^{3+} ions increases the hopping rate of electrons between Fe^{3+} and Fe^{2+} ions at the octahedral site and thus leads to the increase in the Dielectric Loss for the doping of Cu^{2+} from 0.2 to 0.4 .

According to Koop's at lower frequencies, the resistivity is high and the principal effect is of the grain boundaries (low resistivity regions). Therefore, the energy required for electron hopping between Fe^{2+} and Fe^{3+} at the grain boundaries is higher and the energy losses are larger [27-28].

International Journal of Innovative Research in Science, Engineering and Technology

(An ISO 3297: 2007 Certified Organization)

Website: www.ijirset.com

Vol. 6, Issue 7, July 2017

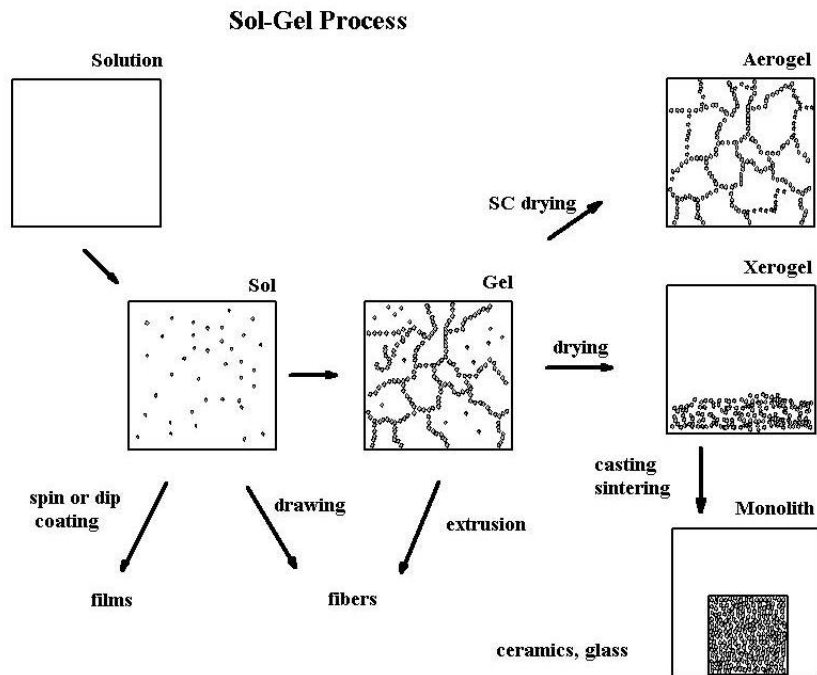


Fig.1: Blocks of SOL GEL for Ferrite Material.

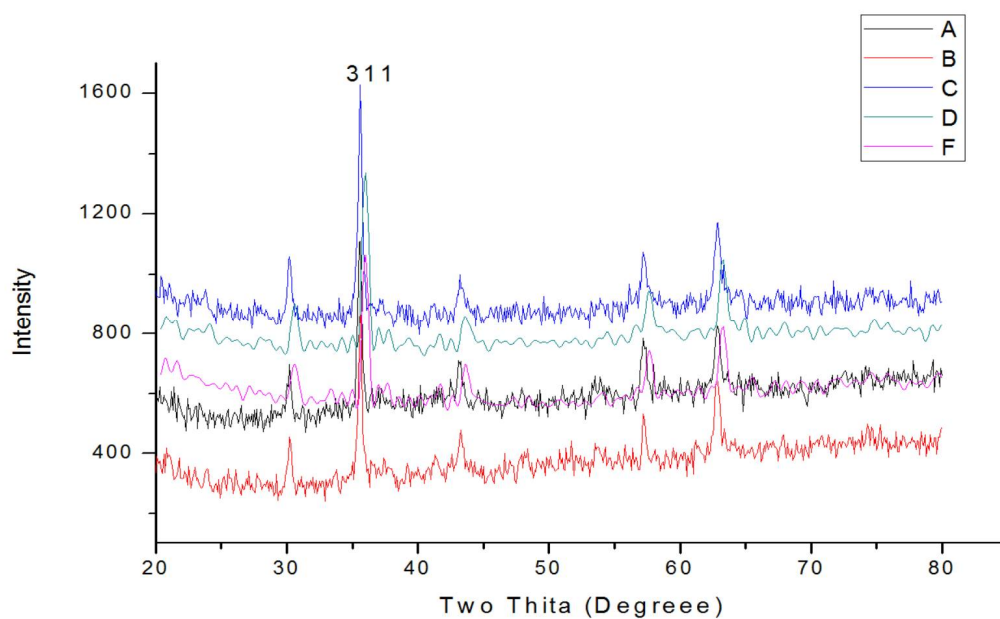


Fig. 2: XRD Pattern of ferrite samples

International Journal of Innovative Research in Science, Engineering and Technology

(An ISO 3297: 2007 Certified Organization)

Website: www.ijirset.com

Vol. 6, Issue 7, July 2017

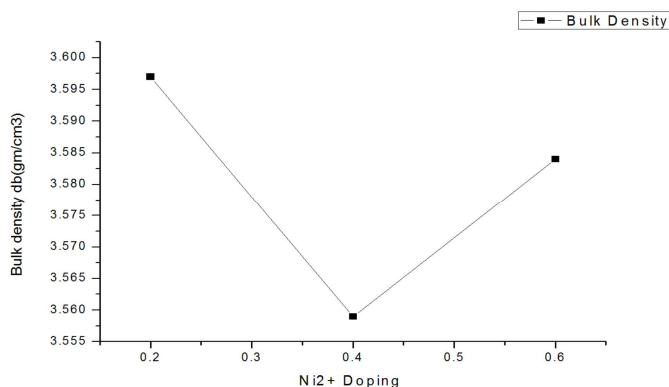
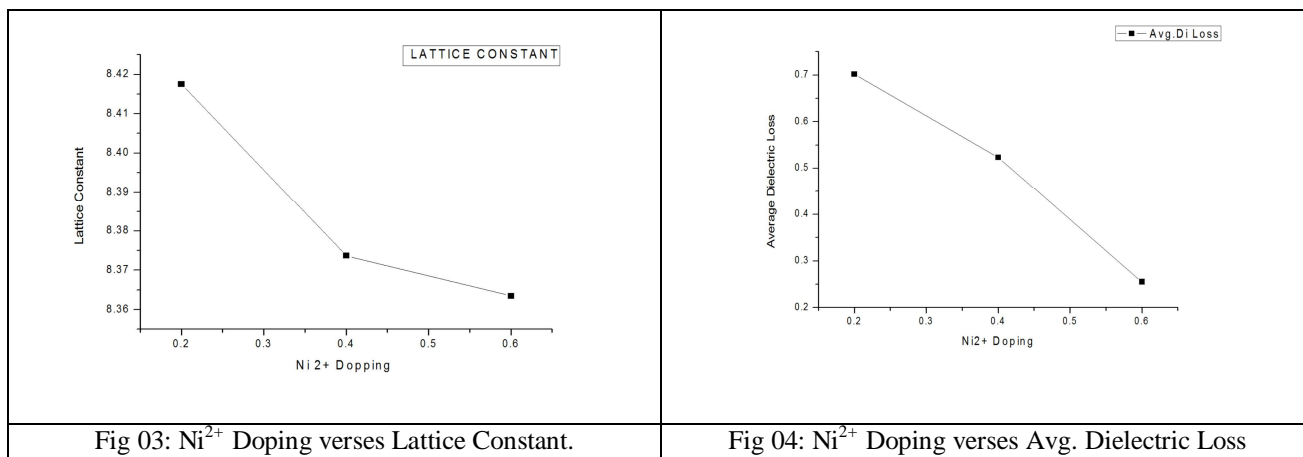
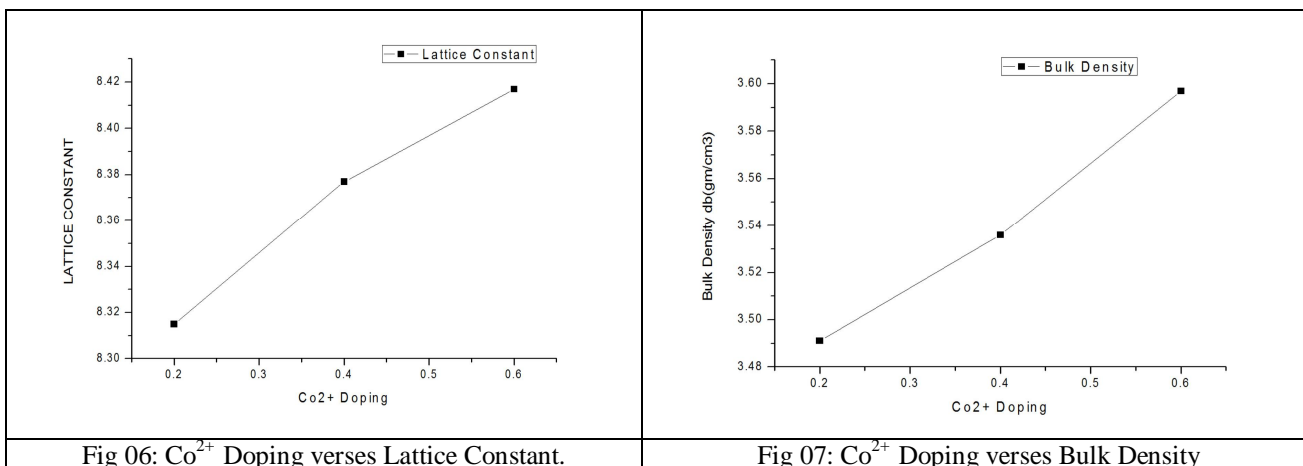


Fig 05: Ni²⁺ Doping versus Bulk Density.



International Journal of Innovative Research in Science, Engineering and Technology

(An ISO 3297: 2007 Certified Organization)

Website: www.ijirset.com

Vol. 6, Issue 7, July 2017

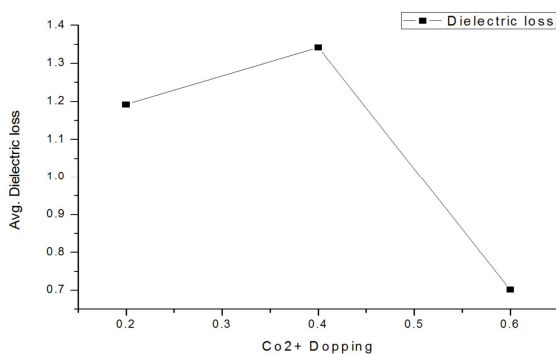


Fig 08: Co²⁺ Doping verses Average Dielectric Loss.

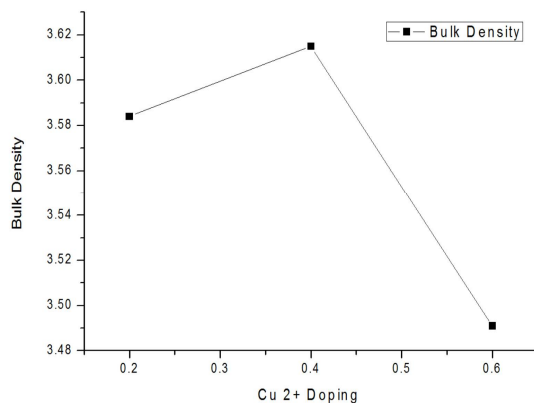
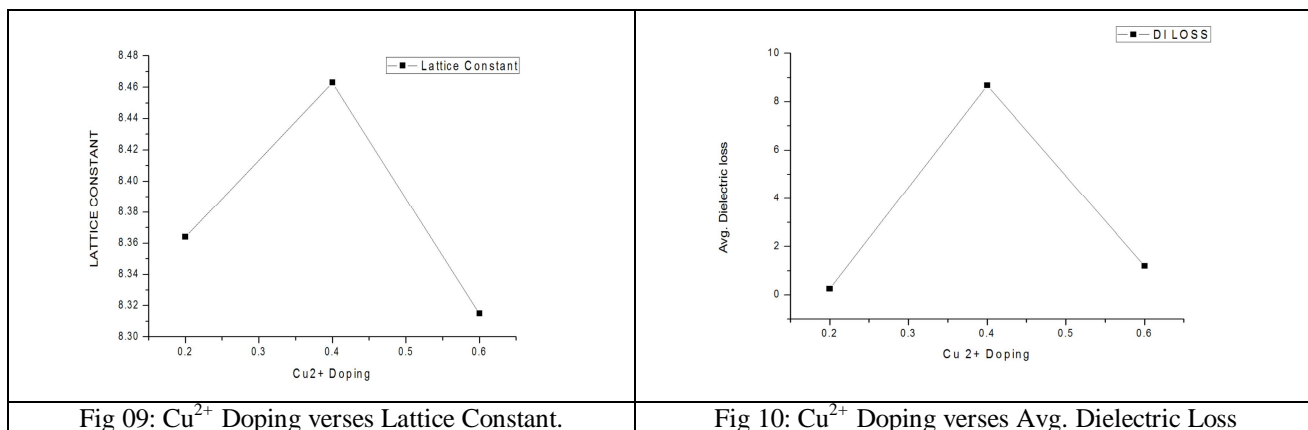


Fig 11: Cu²⁺ Doping verses Bulk Density.

International Journal of Innovative Research in Science, Engineering and Technology

(An ISO 3297: 2007 Certified Organization)

Website: www.ijirset.com

Vol. 6, Issue 7, July 2017

Table 1: Label and Composition of Ferrite Material.

SET	Label	Ferrite Material
SET-I	A	$[(\text{Ni}_{0.2}\text{Cu}_{0.2}\text{Co}_{0.6})\text{Fe}_2\text{O}_4]$
	B	$[(\text{Ni}_{0.4}\text{Cu}_{0.2}\text{Co}_{0.4})\text{Fe}_2\text{O}_4]$
	C	$[(\text{Ni}_{0.6}\text{Cu}_{0.2}\text{Co}_{0.2})\text{Fe}_2\text{O}_4]$
SET-II	D	$[(\text{Ni}_{0.2}\text{Cu}_{0.6}\text{Co}_{0.2})\text{Fe}_2\text{O}_4]$
	E	$[(\text{Ni}_{0.2}\text{Cu}_{0.4}\text{Co}_{0.4})\text{Fe}_2\text{O}_4]$
	A	$[(\text{Ni}_{0.2}\text{Cu}_{0.2}\text{Co}_{0.6})\text{Fe}_2\text{O}_4]$
SET-III	C	$[(\text{Ni}_{0.6}\text{Cu}_{0.2}\text{Co}_{0.2})\text{Fe}_2\text{O}_4]$
	F	$[(\text{Ni}_{0.4}\text{Cu}_{0.4}\text{Co}_{0.2})\text{Fe}_2\text{O}_4]$
	D	$[(\text{Ni}_{0.2}\text{Cu}_{0.6}\text{Co}_{0.2})\text{Fe}_2\text{O}_4]$

Table 2: Bulk Density, Lattices Constant (Å) and Avg. Dielectric loss of All Ferrite Samples (A to F).

Ferrite Sample	Bulk Density	Lattices Constant (Å)	Avg. Dielectric loss
A	3.597	8.417	0.701638
B	3.559	8.374	0.523853
C	3.584	8.364	0.255394
D	3.491	8.315	1.191974
E	3.536	8.377	1.342013
F	3.615	8.463	8.680219

Table 3: Bulk Density, Lattices Constant (Å) and Avg. Dielectric loss due to Ni^{2+} doping for SET-I Ferrite Samples.

Ferrite Sample	Bulk Density	Lattices Constant (Å)	Avg. Dielectric loss
A	3.597	8.417	0.701638
B	3.559	8.374	0.523853
C	3.584	8.364	0.255394

Table 4: Bulk Density, Lattices Constant (Å) and Avg. Dielectric loss due to Co^{2+} doping for SET-II Ferrite Samples.

Ferrite Sample	Bulk Density	Lattices Constant (Å)	Avg. Dielectric loss
D	3.491	8.315	1.191974
E	3.536	8.377	1.342013
A	3.597	8.417	0.701638

Table 5: Bulk Density, Lattices Constant (Å) and Avg. Dielectric loss due to Cu^{2+} doping for SET-III Ferrite Samples.

Ferrite Sample	Bulk Density	Lattices Constant (Å)	Avg. Dielectric loss
C	3.584	8.364	0.255394
F	3.615	8.463	8.680219
D	3.491	8.315	1.191974

IV. CONCLUSION

All ferrite materials are having particle size in nanometer range and exhibit good Dielectric Loss ($\tan \delta$). Ferrite materials can use as electromagnetic wave absorber, core in transformer as well as fabricating antenna and as dielectric

International Journal of Innovative Research in Science, Engineering and Technology

(An ISO 3297: 2007 Certified Organization)

Website: www.ijirset.com

Vol. 6, Issue 7, July 2017

material in capacitors. Sol Gel Auto combustion method is successfully implemented and six different types of Nanocrystalline Ferrite materials successfully prepared.

REFERENCES

- [1] C. G. Whinfrey, D. W. Eckort and A. Tauber, *J. Am. Chem. Soc.* 53 (1982) 2722
- [2] C. Caizer, M. Stefanescu, *J. Phys. D. Appl. Phys.* 35 (2002) 3035
- [3] M.A. Ahmed, S.F. Mansour, M. Afifi, *J. Magn. Magn. Mater.* 324 (2012) 4-10
- [4] P.S. Aghav, V.N. Dhage, M.L. Mane, D.R. Shengule, R.G. Dorik, K.M. Jadhav, *Physica B: Cond. Matter.* 406(2011) 4350
- [5] S. Sun, C.B. Murray, D. Weller, L. Folks, A. Moser, *Science* 287 (2000) 1989
- [6] I.H. Gul, W. Ahmed, A. Maqsood, *J. Magn. Magn. Mater.* 320 (2008) 270-275
- [7] K. Byrappa, M. Yoshimura, Handbook of Hydrothermal Technology, Noyes Publications, New Jersey, USA, 2001.
- [8] P. Hermankova, M. Hermanek, R. Zboril, *Eur. J. Inorg. Chem.*, 2010, 1, 110.
- [9] J. Moulder, Handbook of X-ray Photoelectron Spectroscopy (XPS), USA 1995.
- [10] D. L. Pavla, G. L. Lampman, G. S. Krlz, J. R. Vyvyan, Introduction to spectroscopy, Brooks/ colecengage learning, 2009.
- [11] K.W. Wagner, *Ann. Phys.* 40 (1913) 817.
- [12] I.T. Rabinkin, Z.I. Novikova, Ferrites, *Izv Acad. Nauk USSR*, Minsk, 1960.
- [13] J.C. Maxwell, Electricity and Magnetism, vol. 1, Oxford University Press, New York (1973), p. 1.
- [14] M. Penchal Reddy, W. Madhuri, N. Ramamanoher Reddy, K.V. Siva Kumar, V.R.K. Murthy, R. Ramakrishna Reddy, Influence of copper substitution on magnetic and electrical properties of MgCuZn ferrite prepared by microwave sintering method, *Mater. Sci. Eng. C* 30 (2010) 1094-1099.
- [15] K. J. Azadmanjiri, H.K. Salehani, M.R. Barati, F. Farzan, Preparation and electromagnetic properties of Ni_{1-x}Cu_xFe₂O₄ nanoparticle ferrites by sol-gel auto-combustion method, *Mater. Lett.* 61 (2007) 84-87.
- [16] M.A. Ahmed, S.F. Mansour, M. Afifi, *J. Magn. Magn. Mater.* 324 (2012) 4-10.
- [17] P.S. Aghav, V.N. Dhage, M.L. Mane, D.R. Shengule, R.G. Dorik, K.M. Jadhav, *Physica B: Cond. Matter.* 406(2011) 4350.
- [18] J. Jing, L. Liangchao, X. Feng, *J. Rare Earths* 25 (2007) 79.
- [19] J. Azadmanjiri, H.K. Salehani, M.R. Barati, F. Farzan, *Mater. Lett.* 61 (2007) 84-87.
- [20] J. Du, Z. Liu, W. Wu, Z. Li, B. Han, Y. Huang, *Mater. Res. Bull.* 40 (2005) 928-935.
- [21] M.R. Anantharaman, S. Sindhu, S. Jagatheesan, K.A. Malini, P. Kurian, *J. Phys. D* 32 (1999) 1801
- [22] T. Nakamura, Y. Okaro, Electromagnetic properties of Mn-Zn ferrite sintered ceramics, *J. Appl. Phys.* 79 (1996) 7129.
- [23] T. Jahanbin, M. Hashim, K. A. Mantori, *J. Magn. Magn. Mater.* 322(2010) 2684-2689.
- [24] G.F. Goya, H.R. Rechenberg, Superparamagnetic transition and local-order in CuFe₂O₄ nanoparticles, *Nanostruct. Mater.* 10 (1998) 1001-1011.
- [25] C. G. Koops, *Phys. Rev.* 83 (1951) 121
- [26] J.S. Upadhyay, S. Devendrakumar, S. Omprakash, *Mater. Sci.* 19 (1996) 513
- [27] A. Verma, T.C. Goyal, R.G. Mendiratta, M.I. Alam, *Mater. Sci. Eng. B* 60 (1999) 156-162
- [28] H. Hsiang, W.S. Chen, Y.L. Chang, F.C. Hsu, F.S. Yen, *Am. J. Mater.* 1 (2011) 40-44.